

**AQUEOUS SUCROSE CONCENTRATION
MEASUREMENT BASED ON MICHELSON
INTERFEROMETER**

TAN HONG KOK

UNIVERSITI SAINS MALAYSIA

2015

**AQUEOUS SUCROSE CONCENTRATION
MEASUREMENT BASED ON MICHELSON
INTERFEROMETER**

by

TAN HONG KOK

**Thesis submitted in fulfillment of the requirements
for the degree of
Master of Science**

FEBRUARY 2015

ACKNOWLEDGEMENTS

I would like to express my gratitude toward everyone who helped me achieved the completion of this research works, especially to my supervisor, Dr. Ahmad Fairuz Omar for his given opportunity to allow me pursue research under his utmost supervision. His professionalism, profound knowledge in optics application and friendliness are what it makes up my source of motivation and beacon of reference to overcome the issues throughout the research project and finally accomplished it.

Sincere thanks to my co-supervisor, Dr. Norzaini Zainal who provided invaluable assistance in terms of resource aid, facility and spiritual encouragement toward this research. Thanks to her, I gained a lot of chances to widen my horizon in the sea of physics knowledge. Along with that, special thanks to Local Knowledge LRGS grant (Project Group 3) with account number 203/PTS/6727004 for financial support.

I would also like to acknowledge Assoc. Prof. Dr. Lim Hwee San as a very helpful temporary supervisor and coordinator during my candidature as a postgraduate student. His relentless effort and generosity to help me get through the hardship is invaluable. As without his assistance, it would be impossible for me to get back to track and continue my research until this stage. My gratitude to him is beyond finite words, and I am deeply indebted to him.

Not to forget, a very warm and gracious thank you to lab mates in all engineering physics laboratory, especially Stephenie Yeoh who has been very kind and helpful in providing valuable assistance. Last but not least, the sincere and utmost appreciation has to be expressed towards my family members, especially my

parents for their continuous support with encouragement, love and moral support throughout my research journey. Thank you for staying with me till the very end. Much appreciated.

TABLE OF CONTENTS

	Page
ACKNOWLEDGEMENTS	ii
TABLE OF CONTENTS	iii
LIST OF TABLES	vi
LIST OF FIGURES	vii
LIST OF ABBREVIATIONS	xi
ABSTRAK	xiii
ABSTRACT	xv
CHAPTER 1 - INTRODUCTION	1
1.1 Optical Interference and Interferometry	1
1.1.1 Michelson Interferometer	5
1.1.1.1 Interference of Coherent Electromagnetic Waves	7
1.1.1.2 Condition Requirement for Inducing Interference	8
1.1.1.3 Interference of Two or Multiple Incoherent Waves	10
1.2 Refraction and Refractometry	10
1.2.1 Refractive Index	11
1.2.2 Snell's Law	12
1.3 Aqueous Sucrose Solution	14
1.3.1 Physical Properties	15
1.3.2 Refractive Index and Concentration	16
1.4 Problem Statement	18
1.5 Scope of Research	18
1.6 Research Objectives	18

1.7	Novelty of This Study	19
1.8	Thesis Outline	19
CHAPTER 2 -LITERATURE REVIEW AND THEORY		21
2.1	Overview of Refractive Index and Concentration Measurement	21
2.2	Interferometer Systems for Parameters Measurement	23
2.2.1	Fabry-Pérot Interferometer	23
2.2.2	Mach-Zehnder Interferometer	25
2.2.3	Optical fibre-based In-Fibre Interferometer	26
2.3	Michelson Interferometer and Sensory Application	31
2.4	Derivation Model in Michelson Interferometer Experiment	35
CHAPTER 3 -EXPERIMENTAL DESIGN AND METHODOLOGY		40
3.1	Research Model and Work Flow	40
3.2	Preparation of Aqueous Sucrose Samples	42
3.3	Instrumentation for Interferometry Study	44
3.3.1	Monochromatic Light Source	45
3.3.2	Optical System Base and Components	46
3.3.3	Cuvette and Cuvette Holder Platform	48
3.4	Experiment Setup	49
3.4.1	Preliminary Experiment on Michelson Interferometer	49
3.4.2	Interferometry Experiment for Refractive Index and Concentration Measurement	50

CHAPTER 4 - RESULTS AND DATA ANALYSIS	54
4.1 Preliminary Interferometry Experimental Result	54
4.2 Interferometry Result of Aqueous Sucrose Samples	59
4.2.1 Low Concentration Aqueous Sucrose Samples Results	60
4.2.2 High Concentration Aqueous Sucrose Samples Results	63
4.3 Regression Analysis on Dark Fringes (Minima) Separation Distance	65
4.3.1 Linear Regression	67
4.3.2 Results	68
4.4 Regression Analysis on Bright Fringes (Maxima) Thickness	75
4.4.1 Destructive Interference Samples Group	76
4.4.2 Constructive Interference Samples Group	78
4.4.3 Summary	81
4.5 Red Component Value Analysis on RGB Profile	84
 CHAPTER 5 CONCLUSION AND FUTURE WORKS	 95
5.1 Conclusion	95
5.2 Future Works	97
 REFERENCES	 99
LIST OF PUBLICATIONS AND CONFERENCE PAPERS	104
APPENDICES	105
APPENDIX A Fringes Result and RGB Profile	105
APPENDIX B RGB Value for Random Point at x-axis	115

LIST OF TABLES

	PAGE
1.1 Physical properties of sucrose solution.	16
3.1 Specification of PAL-3 Refractometer (ATAGO, 2014).	44
3.2 Specification of JDSU 1101P He-Ne red laser (JDSU, 2010).	46
4.1 RGB result measurement on preliminary experiment.	55
4.2 RGB result measurement on verification experiment.	58
4.3 Measurement of minima separation distances, X.	69
4.4 Measurement of bright fringe (maxima) thickness for destructive interference.	77
4.5 Measurement of bright fringe (maxima) thickness for constructive interference.	79
4.6 RGB value for 400 th and 500 th horizontal axis pixel position.	86
4.7 Calculated R^2 and RMSE value for regression of random pixels combination.	87

LIST OF FIGURES

	PAGE
1.1 Two monochromatic electromagnetic waves from same coherent source superimpose with each other.	2
1.2 Constructive interference occur when two in-phase wave Superimpose.	2
1.3 Destructive interference occur when two totally out of phase wave superimpose.	3
1.4 Young's Double Slit Experiment (Wolfe, 2011).	3
1.5 Electromagnetic wave geometry of Young's Double Slit Experiment.	4
1.6 Light path geometry in thin film interference.	4
1.7 Mechanism of Newton's Ring formed by air wedge.	5
1.8 Geometrical path of beam propagation in Michelson Interferometer.	6
1.9 Bending of light when entering prism depicting refraction.	11
1.10 Propagation of light path obeys Snell's Law.	13
1.11 Total internal reflection occurred when incident light travel from a medium of lower RI (n_1) to another medium with higher RI (n_2) with incident angle equal or larger than critical angle θ_c .	14
1.12 Molecular structure of sucrose.	15
1.13 Graph depicts relationship between refractive index and concentration level (%Brix or w/w) of aqueous sucrose solution at 20°C (Hanson, 2003).	17
1.14 Temperature dependence of refractive index (Subedi <i>et al.</i> , 2006).	17
2.1 Fabry-Pérot Interferometer.	24
2.2 Mach-Zehnder Interferometer.	26
2.3 Fibre optic MZI interferometric waveguide configuration.	28
2.4 Experimental system setup of fibre optic MZI with a MI addition	29
2.5 Schematic design of MZI variant using unclad optical fibres.	29
2.6 Experimental setup for double interferometer with sliding mirrors.	31

2.7	Michelson Interferometer	32
3.1	Chronological work flow for this research work.	41
3.2	Water sucrose sample preparation (a) Water sucrose samples and (b) sucrose solid material.	42
3.3	Top view of ATAGO PAL-3 Refractometer.	43
3.4	JDSU He-Ne red laser with power supply unit.	45
3.5	Optical components on optical breadboard base.	47
3.6	Cuvette and cuvette holder.	48
3.7	Schematic diagram of Michelson Interferometer experiment setup with path lengths.	50
3.8	Photograph of modified Michelson Interferometer setup.	51
4.1	Default interference fringes pattern and RGB profile.	54
4.2	Verification result for preliminary experiment.	57
4.3	Statistical test of equal variance.	58
4.4	Fringes result of 0% (clear filtered water) sample and RGB profile.	60
4.5	Fringes result of 5 %Brix aqueous sucrose sample and RGB profile.	60
4.6	Fringes result of 10 %Brix aqueous sucrose sample and RGB profile.	61
4.7	Fringes result of 15 %Brix aqueous sucrose sample and RGB profile.	61
4.8	Fringes result of 20 %Brix aqueous sucrose sample and RGB profile.	61
4.9	Fringes result of 25 %Brix aqueous sucrose sample and RGB profile.	62
4.10	Fringes result of 30 %Brix aqueous sucrose sample and RGB profile.	62
4.11	Fringes result of 32 %Brix aqueous sucrose sample and RGB profile.	64
4.12	Fringes result of 40 %Brix aqueous sucrose sample and RGB profile.	64
4.13	Fringes result of 42 %Brix aqueous sucrose sample and RGB profile.	64
4.14	Fringes result of 50 %Brix aqueous sucrose sample and RGB profile.	65
4.15	Demonstration of measurement for minima fringe separation (X_1 , X_2).	67

4.16	Graph of average minima separation distance, X_{avg} versus sample solution concentration.	70
4.17	Calculated concentration against actual concentration of 0 - 50 %Brix aqueous sucrose sample for both minima separation.	70
4.18	Calculated concentration against actual concentration of 0 – 30 %Brix aqueous sucrose sample for both minima separation.	71
4.19	Calculated concentration against actual concentration of 20 – 50 %Brix aqueous sucrose sample for both minima separation.	72
4.20	Calculated concentration against actual concentration of 0 – 50 %Brix aqueous sucrose sample for average of both minima separation.	73
4.21	Calculated concentration against actual concentration of 0 – 30 %Brix aqueous sucrose sample for average of both minima separation.	73
4.22	Calculated concentration against actual concentration of 20 – 50 %Brix aqueous sucrose sample for average of both minima separation.	74
4.23	Demonstration of measurement for maxima fringe thickness (d_1 and d_2).	75
4.24	Graph of average maxima thickness versus sample solution concentration for destructive interference samples group.	76
4.25	Calculated concentration against actual concentration of destructive interference aqueous sucrose sample group for both maxima thickness reading.	78
4.26	Graph of average maxima thickness versus sample solution concentration for constructive interference samples group.	80
4.27	Calculated concentration against actual concentration of constructive interference aqueous sucrose sample group for both maxima thickness readings.	80
4.28	Graph of average maxima fringe thickness versus sample solution concentration of 0 - 50 %Brix.	81
4.29	Calculated concentration against actual concentration of 0- 50 %Brix aqueous sucrose for all average maxima thickness readings.	82
4.30	Calculated concentration against actual concentration of 0 – 30 %Brix aqueous sucrose for all average maxima thickness readings.	83
4.31	Calculated concentration against actual concentration of 32 -50 %Brix aqueous sucrose for all average maxima thickness readings.	83

4.32	Calculated concentration against predicted actual concentration of 0-50%Brix aqueous sucrose samples for red color value at random of horizontal axis pixel positions (400, 500, 600, 700, 800, 1000, 1200, 1400, 1600, 1800).	88
4.33	Calculated concentration against predicted actual concentration of 0 - 50%Brix aqueous sucrose samples for red color value at random of horizontal axis pixel positions (800, 1000, 1200, 1400, 1600, 1800, 1900, 2000, 2100, 2200).	89
4.34	Calculated concentration against predicted actual concentration of 0 – 50 %Brix aqueous sucrose samples for red color value at random of horizontal axis pixel positions (400, 500, 600, 700, 800, 1800, 1900, 2000, 2100, 2200).	90
4.35	Calculated concentration against predicted actual concentration of 0 - 50 %Brix aqueous sucrose samples for red color value at random of horizontal axis pixel positions (600, 700, 800, 1000, 1200, 1400, 1600, 1800, 1900, 2000).	91
4.36	Calculated concentration against predicted actual concentration of 0 – 50 %Brix aqueous sucrose samples for red color value at random of horizontal axis pixel positions (400, 500, 600, 800, 1200, 1600, 1800, 2000, 2100, 2200).	92
4.37	Calculated concentration against predicted actual concentration of 0 – 50 %Brix aqueous sucrose samples for red color value at random of horizontal axis pixel positions (400, 600, 800, 1000, 1200, 1400, 1600, 1800, 2000, 2200).	93

LIST OF ABBREVIATIONS

AR	= Anti-Reflective
CCD	= Charge-Coupled Device
DSLR	= Digital Single Lens Reflective
EM	= Electromagnetic
FPI	= Fabry-Perot Interferometer
FBG	= Fiber Bragg Grating
FFPI	= Fiber Fabry-Perot Interferometer
FWHM	= Full Width at Half Maximum
He-Ne	= Helium-Neon
LPFG	= Long Period Fiber Grating
MI	= Michelson Interferometer
μL	= micro litre
MZI	= Mach-Zehnder Interferometer
nm	= nanometer
OPL	= Optical Path Length
OPD	= Optical Path Difference
PLS	= Partial Least Square
$\Delta\phi$	= Phase Difference
R^2	= R-Square
RI	= Refractive Index
RGB	= Red, Green and Blue
RMSE	= Root Mean Square Error
SMF	= Single Mode Fiber
SO ₂	= Sulphur Dioxide

TIR = Total Internal Reflection

k = Wave Constant

w/w = weight/weight

PENYUKATAN KEPEKATAN LARUTAN BERAIR SUKROSA MELALUI MICHELSON INTERFEROMETER

ABSTRAK

Penyukatan kepekatan bagi larutan berair adalah secara terus bergantung kepada indeks biasan (RI) medium berair yang berfungsi sebagai faktor dominan. Pemahaman sifat perubahan dalam nilai RI adalah penting untuk mengukur kepekatan sampel berair dengan tepat. Oleh sebab tahap ketepatan pengukuran RI yang amat tinggi (sehingga 5 tempat perpuluhan) pada masa kini, peralatan yang mempunyai sifat kepekaan yang tinggi diperlukan untuk membuat pengukuran yang tepat. Objektif utama penyelidikan ini adalah untuk membangunkan satu sistem Michelson interferometer (MI) yang berdasarkan konsep interferometri untuk menyukat tahap kepekatan sampel berair sukrosa dan juga menentukan hubungan antara RI dan tahap kepekatan sampel. Dalam kajian ini, analisis kuantitatif dijalankan ke atas 41 sampel sukrosa berair (termasuk air paip yang ditapis) yang terdiri daripada tahap kepekatan yang berbeza di antara 0% hingga 50% Brix dengan meletakkan sampel berair sukrosa di dalam sel kuarza padu yang membolehkan pancaran laser menembusnya dan menghasilkan corak interferens melalui MI. Hasil imej corak interferens yang terhasil akan direkod dan diproses dengan menggunakan perisian pemprosesan imej. Nilai warna merah, hijau, biru (RGB) yang diperolehi melalui perisian digunakan untuk mengira nilai jarak pemisahan antara pinggir gelap, nilai ketebalan pinggir cerah, dan juga analisis profil RGB berdasarkan titik-titik secara rambang. Analisis yang berlainan dijalankan terhadap golongan sampel kepekatan tinggi dan golongan sampel kepekatan rendah boleh didapati di dalam isi kandungan. Secara kesuluruhannya daripada pencarian penyelidikan, jarak pemisahan pinggir gelap dan ketebalan piggir cerah menunjukkan nilai regresi R-kuasa dua (R^2) masing-masing sebanyak 88.90% dan 55.54%. Hasil daripada eksperimen

menunjukkan keputusan yang baik dan agak sejajar dengan ramalan teori dan kesimpulanya adalah nilai RI akan meningkat dengan penambahan kepekatan larutan berair dengan berkadar linear.

AQUEOUS SUCROSE CONCENTRATION MEASUREMENT BASED ON MICHELSON INTERFEROMETER

ABSTRACT

Measurement of concentration for aqueous solution is fundamentally relied on the refractive index (RI) of the aqueous medium as a dominant factor. Understanding the nature of variation for RI is crucial for precise measurement of solution concentration. Due to the high precision level of RI (up to 5 decimal places) nowadays, a high sensitivity versatile instrument such as optical interferometer is required to enable accurate measurement. The main objective of this research work is to develop a non-destructive Michelson Interferometer (MI) based interferometry setup to measure the concentration level of aqueous sucrose samples and as well as investigate the correlation between RI and concentration level of the samples. In this research, quantitative analysis of 41 aqueous sucrose samples (including 0 %Brix clear filtered water) with different concentration level ranging from 0% to 50 %Brix are accomplished by allocating the aqueous samples in a cubic quartz cuvette to allow the transmission of laser pass through and produce interference fringes as a result of going through MI. Image result of the interference patterns generated are captured and processed with the help of image processing software. Red, green, blue (RGB) gray value obtained is used to calculate multiple minima (dark fringe) separations, maxima (bright fringe) thickness values, and as well as RGB profile analysis based on random pixel points. Independent analysis of low concentration samples segment and high concentration samples segment in respective order are available in the content. From the research, the minima separations and maxima thickness show fair regression response in R-squared (R^2) value of 88.90% and 55.54% respectively. The findings from experiment depict good agreement with

theoretical prediction and can be concluded with the RI response proportionally to aqueous solution concentration in linearly ascending order.

CHAPTER 1

INTRODUCTION

Optics is the branch of physics which study about the nature of light from scientific aspect. Thus, study of optics involved a very broad topic coverage including the interaction of light with matter. Generally under the linear optics, there are geometric optics and physical optics. Geometric optics study light travel in straight lines and light undergoes refraction and reflection, while physical optics study light as properties of wave such as diffraction and interference. Light is an electromagnetic waves. Therefore, studying optics also related to other electromagnetic waves such as X-ray, infrared ray and microwaves.

1.1 Optical Interference and Interferometry

Interference of wave is a phenomenon due to superposition of two mechanical waves. The two waves can be added constructively when they are in phase, the amplitude of resultant wave is greater than each individual waves, it is called as constructive interference; whereas when two waves are out of phase, destructive interference happens and the amplitude of resultant wave will be less (Morin, 2010). The resultant wave at any point within region where waves superimposed is the vector sum of each wave (Iyer, 2006). To observe phenomenon of interference of waves, the waves can add constructively if they are in phase, or destructively if they are out of phase, or something in between for other phases. To observe phenomenon of interference of waves from two sources, the two sources must be monochromatic and coherent (Serway & Jewett, 2014).

Optical interference can be produced by a number of types of optical instruments and these instruments are grouped under the generic name of interferometer. Interferometers are basic optical tools used to precisely measure wavelength, distance, index of refraction, and temporal coherence of optical beams. Most modern interferometers use laser light as it's more regular and precise compare to ordinary light, in addition to produce coherent beams in which all the light waves travel in phase. The family of interferometers includes Fabry-Perot interferometer (FPI), Fizeau interferometer (FI), Twyman-Green interferometer (TGI), Mach Zehnder interferometer (MZI) and not forgetting the long existing, well-known Michelson interferometer (MI) used in the famous Michelson-Morley experiment (Woodford, 2014).

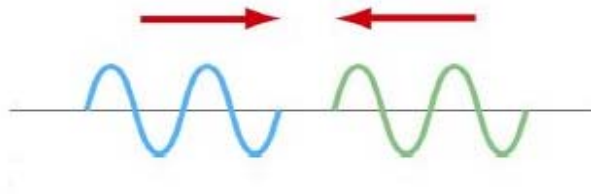


Figure 1.1 Two monochromatic electromagnetic waves from same coherent source superimpose with each other.

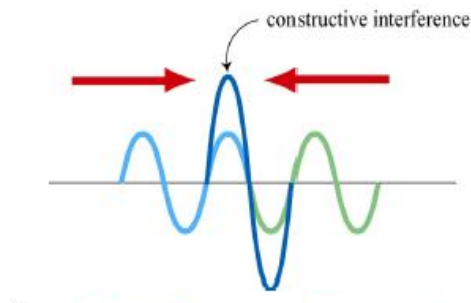


Figure 1.2 Constructive interference occur when two in-phase wave superimpose.

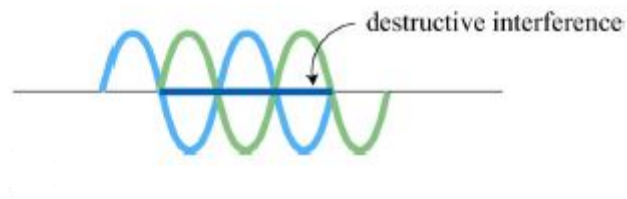


Figure 1.3 Destructive interference occur when two totally out of phase wave superimpose.

Young first demonstrated his famous Young Double Slit Experiment in 1801 (Zappe, 2010). Figure 1.4 and Figure 1.5 shows the geometry setup of Young Double Slit Experiment. It is basically an interferometer based on double-slit setup, where the propagating wavefronts are generated from the aperture slit interfering among each other. The monochromatic light source is incidence to S_0 and pass through two slits S_1 and S_2 to form the interference pattern on the screen.

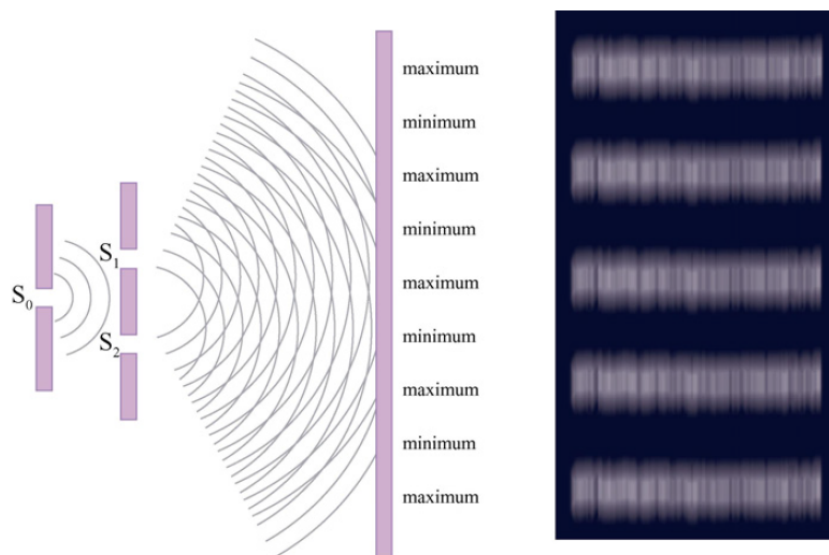


Figure 1.4 Young's Double Slit Experiment (Wolfe, Hatsidimitris, & Smith, 2014)

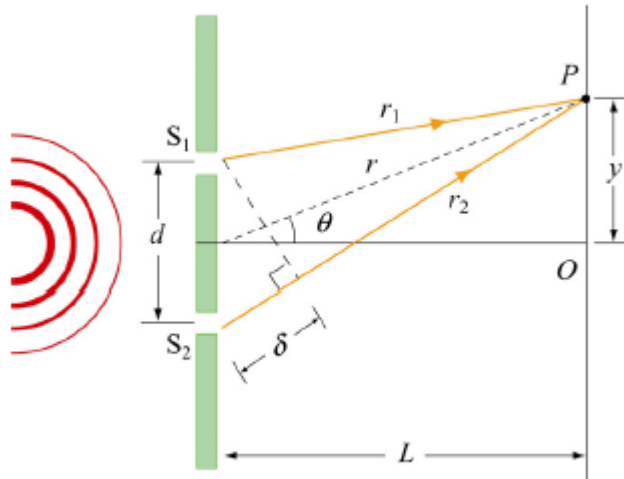


Figure 1.5 Electromagnetic wave geometry of Young's Double Slit Experiment.

Interference of light can also easily be seen by interference of thin film. Figure 1.6 shows the light travelling in a thin film causing interference. Light entering multiple layers of substance medium will undergo refractions and internal reflections, whereby the reflection light waves transmitted into observation spot are travelling marginally close enough to overlap each another and cause interference.

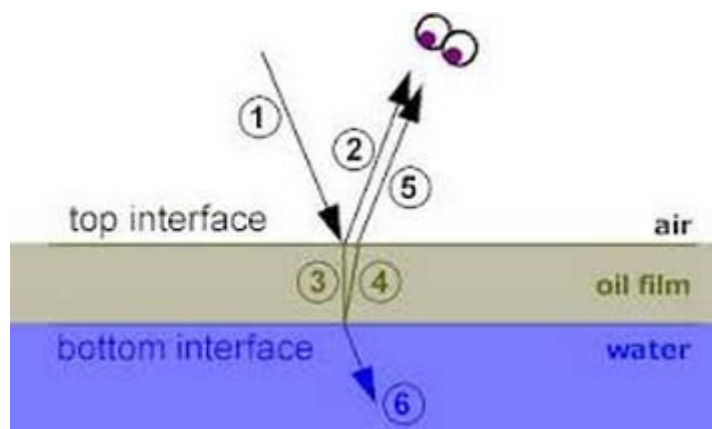


Figure 1.6 Light path geometry in thin film interference.

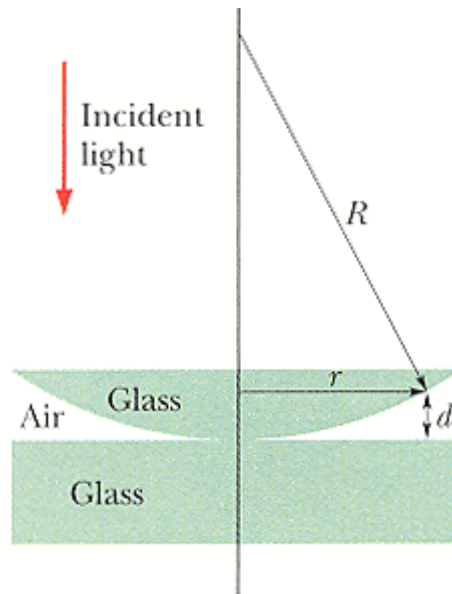


Figure 1.7 Mechanism of Newton's Ring formed by air wedge.

Another method for observing interference of light is by placing a plano-convex lens on top of a flat glass surface and the interference pattern formed is called Newton's Ring as shown in Figure 1.7 (Serway & Jewett, 2014).

1.1.1 Michelson Interferometer

The Michelson interferometer (MI), which was developed by Albert Michelson in 1881, with great historical significance, has contributed a lot in modern physics and nonetheless is an optical instrument of high precision and versatility. This versatile instrument was used to establish experimental evidence for the development for the validity of the special theory of relativity, to detect and measure hyperfine structure in line spectra, to measure the tidal effect of the moon on the earth and to provide a substitute standard for the meter in terms of wavelengths of light. In the history timeline, this instrument was used by Michelson and Morley to try and measure the Doppler shift of light travelling parallel to and perpendicular to the motion of earth

through the ether. The result of the Michelson-Morley experiment that disproved the existence of ether became the stepping stone toward Albert Einstein's theory of relativity and eventually leads to the revolution in physics at the beginning of the twentieth century (Iyer, 2006).

The MI causes interference by splitting a beam of light into two so that one beam strikes a fixed mirror and the other a movable mirror. Each part of the transmission light is made to travel at a different path of length difference so that a single interference pattern results appear when the reflected beam are brought back together.

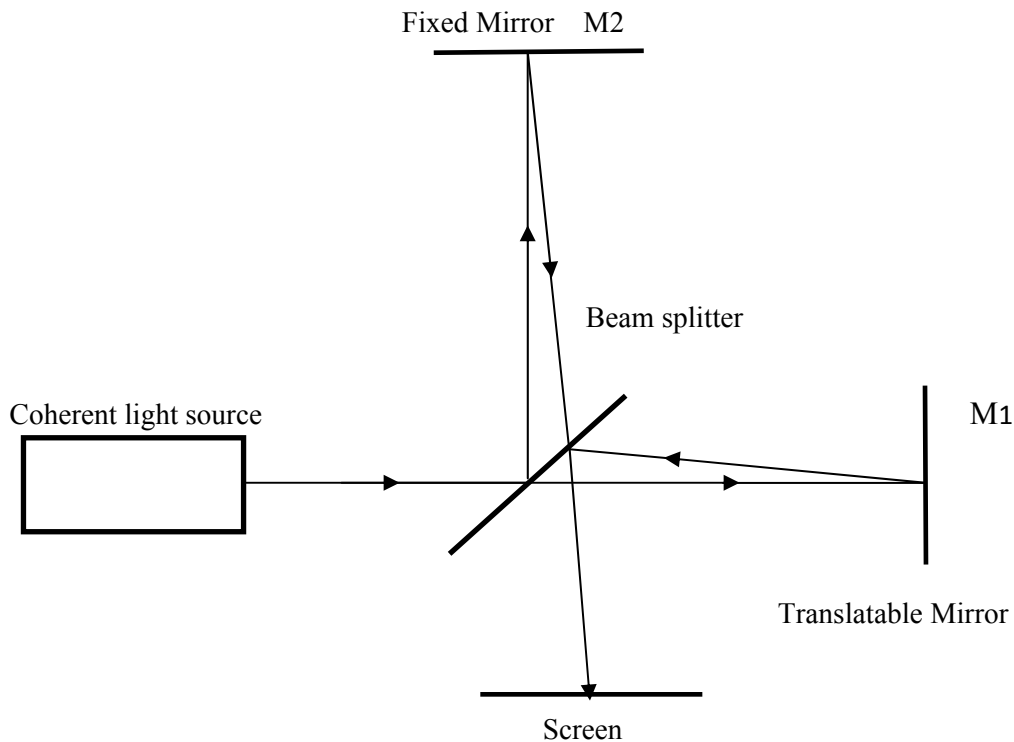


Figure 1.8 Geometrical path of beam propagation in Michelson Interferometer.

Figure 1.8 depicts the fundamental design of typical MI with detailed travelling geometrical light path showing the operation mechanism. The MI operates on the principle of division of amplitude rather than on division of wavefront. Light from a light source strikes the beam splitter and is split into two parts. The beam

splitter allows 50% of the radiation to be transmitted to the translatable mirror M_1 . The other 50% of the radiation is reflected back to the fixed mirror M_2 . Both these mirrors, M_1 and M_2 , are highly silvered on their front surfaces to avoid multiple internal reflections. After returning from M_1 , 50% of the light is reflected toward the frosted glass screen. Likewise, 50% of the light returning from M_2 is transmitted to the glass screen. The two beams are superposed and one can observe the interference fringe pattern on the screen. The character of the fringes is directly related to the different optical path lengths traveled by the two beams and therefore is related to whatever causes a difference in the optical path lengths (Iyer, 2006).

Precise distance measurements can be made with the MI by moving the mirror and counting the interference fringes which move by a reference point. The distance, d associated with m fringes is:

$$d = \frac{m\lambda}{2} \quad (1.1)$$

1.1.1.1 Interference of Coherent Electromagnetic Waves

Principle of superposition states that when two Electro-Magnetic (EM) waves simultaneously propagate through the same region of space, the resultant electric field at any point in that region is the vector sum of the electric field of each wave. If two beams emanate from a common single source, but travel over two different geometrical paths to a destination spot or a detector, the field at the corresponding spot will be determined by the optical path difference, which we will denote by:

$$\Delta x = x_2 - x_1 \quad (1.2)$$

So if two waves of the same frequency, ω , but of different amplitude and different phase impinge on one point they are superimposed, or interfere, so that:

$$y = a_1 \sin(\omega t - \alpha_1) + a_2 \sin(\omega t - \alpha_2) \quad (1.3)$$

where a_1 and a_2 are the amplitudes of both the waves and α_1 and α_2 are the phase angles at any time, t .

The resulting wave can be described as

$$y = A \sin(\omega t - \alpha) \quad (1.4)$$

with A being the resultant amplitude and α the resultant phase.

$$A^2 = a_1^2 + a_2^2 + 2a_1a_2 \cos\Delta\phi \quad (1.5)$$

where $\Delta\phi$ is the phase difference which is given by:

$$\Delta\phi = \alpha_1 - \alpha_2 = \frac{2\pi}{\lambda} \Delta x \quad (1.6)$$

where λ is the wavelength of the light source used.

1.1.1.2 Condition Requirement for Inducing Interference

In order for optical interference to occur, several conditions are required to present and fulfill. First of all, the light source must be monochromatic, which means the light beam must only possess a single wavelength (λ) or frequency. Under the usual condition, the light sources must also remain spatially coherent (constant phase difference) with each of them. Amplitudes of two waves having interference are required to be approximately equal to each other so that general illumination can be

avoided. Light interference will result in two different phases, namely constructive interference and destructive interference.

Constructive interference occurs when

$$\Delta\varphi = 2m\pi, m = 0, \pm 1, \pm 2, \pm 3 \quad (1.7)$$

Based on the different light paths, the phase difference is:

$$\Delta\varphi = \frac{2\pi}{\lambda} \Delta x = \frac{2\pi}{\lambda} 2d \cos \theta \quad (1.8)$$

Comparing both equations:

$$2d \cos \theta = m\lambda ; m = 0, \pm 1, \pm 2, \pm 3 \quad (1.9)$$

in which circles are produced for a fixed value of m and d since θ remains constant for a perfect beam alignment scenario. In the case of realistic situation where there will be always some slight misalignment of superposition beams, straight “fringes with equal thickness” will appear instead of the circular fringes. So if both the optical path lengths are the same or if these two paths differ by an integral number of wavelengths λ , the condition for constructive interference is met. Thus, bright fringes will be formed for that wavelength.

On the other hand, the condition for destructive interference is met when the two optical paths differ by an odd integral number of half wavelengths $\frac{m}{2}\lambda$ where $m = 0, \pm 1, \pm 2, \pm 5$ and so on. Thus, dark fringes will be formed and destructive interference occurs at:

$$\Delta\varphi = \pm(2m + 1)\pi, m = 0, 1, 2, 3 \quad (1.10)$$

1.1.1.3 Interference of Two or Multiple Incoherent Waves

Optical interference can also occur in the case of two out-of-phase waves superimpose with each other, given under special condition. Consider the case of two frequencies with wavenumbers k_1 and k_2 that together follow two different paths with a difference of Δx . The sum of the waves with different amplitudes at point x along the x -axis is given by:

$$E_T = (e^{ixk_1} + e^{i(x+\Delta x)k_1})E_1 + (e^{ixk_2} + e^{i(x+\Delta x)k_2})E_2 \quad (1.11)$$

If $a = \frac{E_2}{E_1}$ and define $\delta k = \frac{(k_1 - k_2)}{2}$, after doing a lot of algebra, the intensity ($E_T \cdot E_T$) can be write as:

$$2(l + a + a^2 + a \cos 2 \delta k \Delta x + (1 + a)(\cos k_1 \Delta x + a \cos k_2 \Delta x)) \quad (1.12)$$

1.2 Refraction and Refractometry

Refraction is a surface phenomenon involving the bending of a wave such as light due to the change in its transmission medium. It involved changes in speed of travelling waves from one medium to another due to difference in refractive index (RI) of both medium. When the ray of light is refracted at the interface of two different medium, the transmitted ray remains within the plane of incidence. The refracted ray is bent towards the normal of the plane when the second medium is denser. Sine of refraction is directly proportional to sine of incidence (Pedrotti, Pedrotti, & Pedrotti, 1993). The phenomenon of refraction is explained by Snell's Law. Figure 1.9 shows some of the optical phenomena caused by refraction.

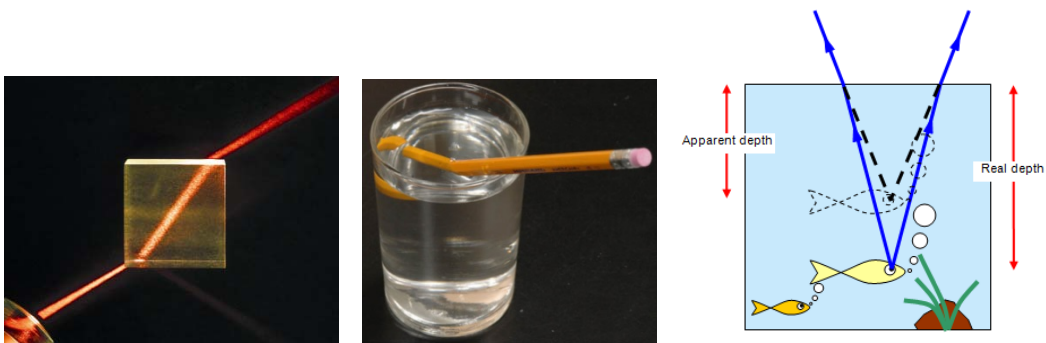


Figure 1.9 Bending of light when entering prism depicting refraction.

1.2.1 Refractive Index

In the world of optics, RI or index of refraction defined as the relative ratio of speed of light, c travelling in a vacuum space medium to the speed of light travelling in a possibly higher density specified medium (Hecht, 2002). RI usually applies on material of the medium to measure the speed of light with given wavelength travelling inside. Refractive index, n is defined as:

$$n = \frac{c}{v} \quad (1.13)$$

where n is the absolute RI of the medium, c is the speed of light, and v is the speed light travelling in the specific medium. The term of absolute RI is used for referring RI of the material in relative to speed of light travelling in true vacuum space, as opposed to relative RI provided for a boundary of two non-vacuum medium (ChemBuddy, 2011). As the value of RI increasing, the slower the light wave propagates inside the corresponding medium.

Generally, RI for most of the solids and aqueous solutions depend on the density of their composition material. The higher the density is for the material, the higher RI they possess. RI is also a temperature dependent variable. In most of the

cases for gas and aqueous substances, RI shares an inverse proportional relation with temperature parameter.

1.2.2 Snell's Law

Snell's law, which refers to the law of refraction in optical context, is used to describe the relationship between the angles of refraction and incident of waves passing through two different medium with different RI. Electromagnetic wave, such as light, abides Snell's Law when it travels from one lesser density medium to another higher density medium (Schechter, 1977).

Historical development of Snell's Law started from Claudius Ptolemaeus, or more commonly known as Ptolemy, with his discovery of refraction angles relativity for models involving small angle values (Harland, 2007). Then, the law of refraction was pioneered by Ibn Sahl, who was the first to publish an accurate description of it in his work "On Burning Mirrors and Lenses" (Rashed, 1990) by making use the derivation of formula to adjust lens' shape for focusing light with no geometric aberration. In 1678, Huygens-Fresnel principle is used to explain Snell's Law by Christiaan Huygens.

The equation of Snell's Law is known as:

$$\frac{\sin \theta_1}{\sin \theta_2} = \frac{v_1}{v_2} = \frac{n_2}{n_1} \quad (1.14)$$

where θ is the angle measured from the normal, v is the velocity of light in the respective medium (in ms^{-1}) and n is the RI of the respective medium. Simplifying the equation terms will yield:

$$n_1 \sin \theta_1 = n_2 \sin \theta_2 \quad (1.15)$$

which is the more widely known of expression form for Snell's Law.

When light travels from one initial medium to another transmitted medium, the velocity of light tends to change so that the ratio of sine of incidence ray and refraction rays is kept constant as shown in Figure 1.10 (Schechter, 1977). This explains why RI of the transmitted medium and the refracted angle of light are inversely proportional, meaning that as the RI of transmitted medium increase, the output refracted angle decrease with respect to normal plane due to the constant ratio had to be maintained.

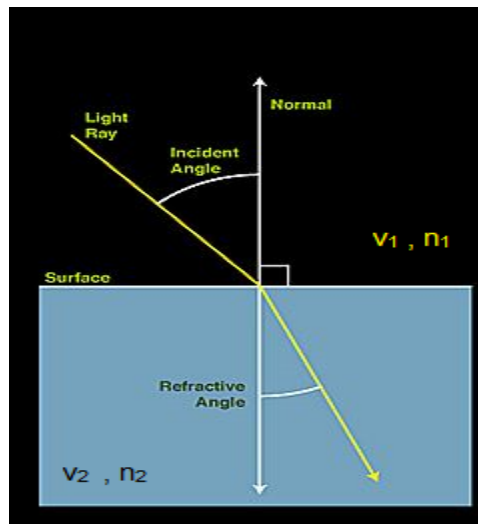


Figure 1.10 Propagation of light path obeys Snell's Law.

However, when incidence rays in a medium of higher RI pass through to a medium of lower RI exceeds critical angle, $\theta_c (\geq 90^\circ)$, total internal reflection (TIR) occurs. When TIR phenomenon occurs, incidence rays will get deflect and bounce off from the boundary surface between two mediums instead of transmit through into another medium.

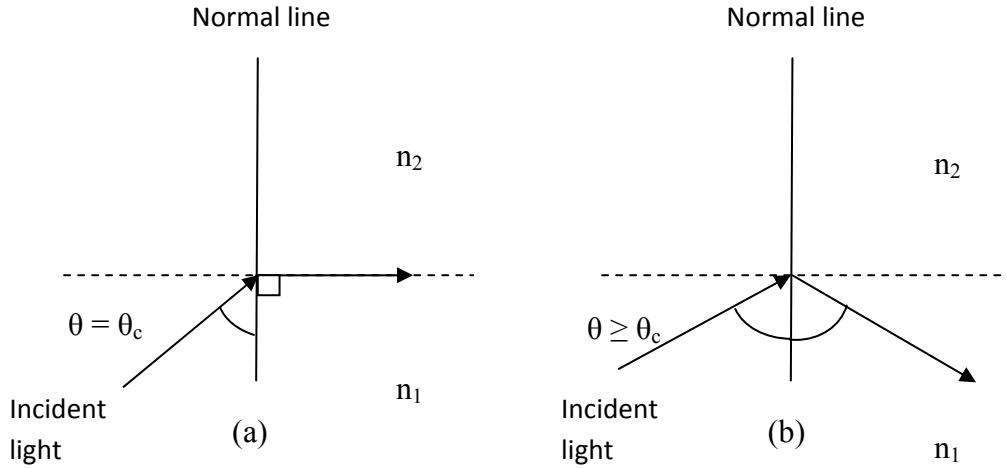


Figure 1.11 Total internal reflection occurred when incident light travel from a medium of lower RI (n_1) to another medium with higher RI (n_2) with incident angle equal or larger than critical angle θ_c .

As shown in Figure 1.11(a), transmitted light reflect and travel perpendicular to normal line when incident angle equal to critical angle θ_c . While for 1.11(b), incident light undergoes TIR at the boundary of two medium when incident angle is larger than to critical angle θ_c .

1.3 Aqueous Sucrose Solution

Aqueous sucrose solution is chosen as a RI samples in this research work due to its transparency properties which allow light beam to go through, and customizable RI based on different level of liquid concentration. Besides that, the easy availability and high solubility characteristic as a material also makes it a good choice of sample.

1.3.1 Physical Properties

Sucrose is a white, odorless, crystalline powder that comes with the sweet taste. It is commonly known as saccharose or generally called as table sugar or cane sugar. The official molecular formula of sucrose is $C_{12}H_{22}O_{11}$. It is a disaccharide composed from monosaccharides which are glucose and fructose. The IUPAC name is (2R,3R,4S,5S,6R)-2-[(2S,3S,4S,5R)-3,4-dihydroxy-2,5-bis(hydroxymethyl)oxolan-2-yl]oxy-6-(hydroxymethyl)oxane-3,4,5-triol. Figure 1.12 shows the molecular structure of sucrose. From Figure 1.12, it shows that sucrose molecules do not contain a free anomeric carbon atom. The physical properties of sucrose are shown in Table 1.1.

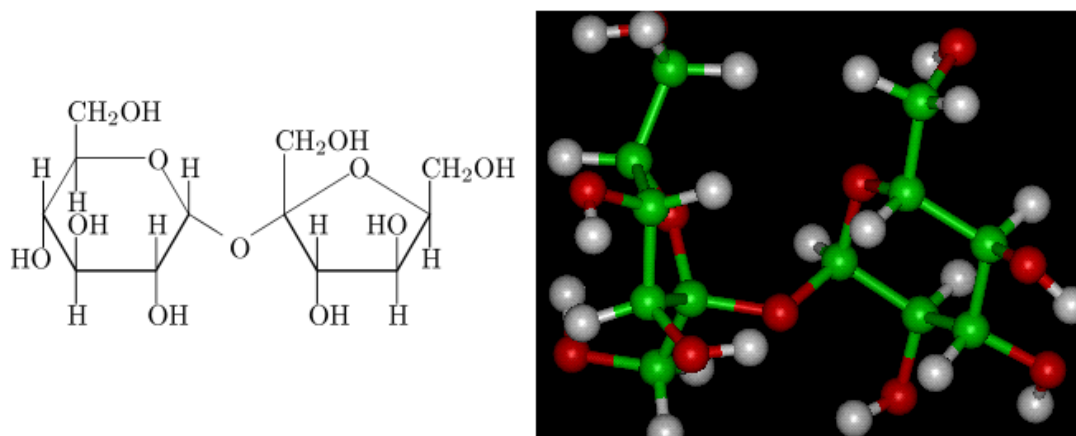
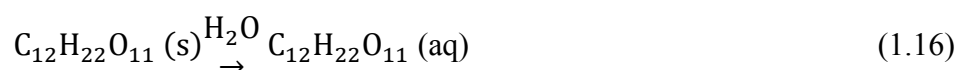


Figure 1.12 Molecular structure of sucrose.

When sucrose solids dissolves in water, molecular solids dissociated and the weak glycosidic bond are broken, causing the sucrose molecule merged into water solution (Bodner, 2014). The equilibria for the process is:



Solubility of sucrose solids improve proportionally with the increase in temperature. This is proven when the solubility of sucrose solids in water is

approximately 2.04 g/mL at 20°C (room temperature), increase exponentially to 4.87 g/mL at temperature of 100°C (StasoSphere, 2014).

Table 1.1 Physical properties of sucrose solution.

Physical properties of Sucrose	Parameter
Molar mass	342.30 g/mol
Density (solid form)	1.587 g/cm ³
Melting/Decomposition point	186 °C (to form caramel, decompose into 1 molecule of glucose and fructose)
Solubility in water	2000 g/L (25 °C)

1.3.2 Refractive Index and Concentration

As a substance, aqueous sucrose solution has specific RI depending on the sugar composition concentration and temperature. Due to rapid development in RI study with high correlation accuracy between each research effort, official reading scale for RI measurement of aqueous sucrose has reached to an advancement region of five decimal places (Charles, 1965). RI values of sucrose solutions are in direct proportion relation with its concentration in term of dissolved solids in soluble reagent. As shown in Figure 1.13, RI of sucrose increase from approximately 1.3344 sat 1 %Brix to 1.4906 at 80 %Brix, given the constant temperature condition at 20°C.

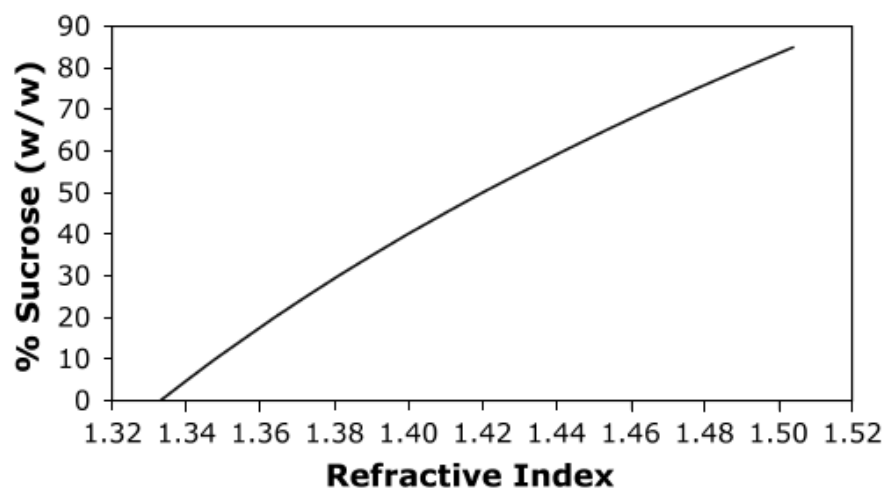


Figure 1.13 Graph depicts relationship between RI and concentration level (%Brix or w/w) of aqueous sucrose solution at 20°C (Hansen, 2003).

Temperature factor plays a major role in affecting absolute RI of aqueous sucrose solution due to expansion of volume in water when the temperature increased. Figure 1.14 shows the relation between RI of water and temperature in degree celcius. Under normal circumstances and conditions, RI of water decrease when temperature of water increase.

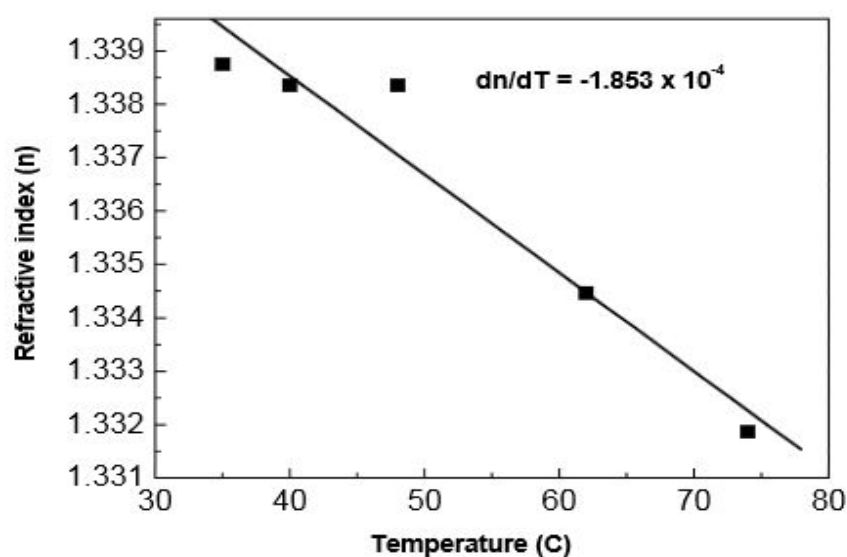


Figure 1.14 Temperature dependence of RI (Subedi *et al.*, 2006).

1.4 Problem Statement

RI and concentration of an aqueous solution, especially water sucrose is not something uncommon to us in everyday life, however, the determination of their relationship and accurate measurement of both the properties are not easy to be carried out under normal circumstances. They involve sophisticated process and instruments that comes with high cost and low availability, which cause difficulty even for average research practitioner to get the hands on. Precise measurement of water sucrose concentration is essential to prevent overtaking of sugar level in our human body, which is detrimental to our health as they can cause diabetes and other associated chronic diseases.

1.5 Scope of Research

This research work emphasizes on the study of interferometry fringes produced in the function of various water sucrose solutions concentrations to determine the absolute RI of it. RI of the water sucrose solutions are determined by the analysis of interference fringes characteristic using image processing software and the accuracy of the measurement is justified by mathematical method of linear regression equation. Verification of measurement system reproducibility is conducted at the final phase to improve the reliability of it.

1.6 Research Objectives

This research study aims to achieve the following objectives:

1. To develop a simple, non-destructive, and user friendly interferometric based device/system for measurement of RI and aqueous solution concentration using Michelson Interferometer as fundamental design basis.
2. To determine the correlation and relationship between water sucrose solution concentration and RI in two-way vice versa approach.
3. To investigate and validate the interferometry method of analysis involving measurement of dark fringes separation and bright fringes thickness

1.7 Novelty of This Study

Studies on the interference fringes properties by the water sucrose solutions will lead a discovery of possible new method to analyse and determine the RI as well as concentration degree (%Brix), which will enhance the accuracy and efficiency of the measurement process. Foundation knowledge of MI system and interference fringes quality acquired through this study may serve as a “step-stone” toward development of interferometer-based holography system.

1.8 Thesis Outline

This thesis consists of five chapters. Chapter 1 introduces the theoretical background involved mainly on optical phenomena and also an overview of the research work conducted. It also includes the problem statements, research objectives, scope of research and the novelty of this work. Chapter 2 presents the literature review which consists of the past and recent works in relative to RI measurement of various subjects in the form of solids, liquids, and gases. Various measurement and analysis approaches are discussed as well. Methods, instruments and work procedures of this

research work are discussed in chapter 3. Chapter 4 presents the results and in-depth data analysis of this study, along with the discussion and validation of the results obtained. Chapter 5 sums up all the progress and output of this study, with additional recommendations for future developments.

CHAPTER 2

LITERATURE REVIEW AND THEORY

In this chapter, information and in-depth review of relevant research articles are mentioned. Discussion of various available interferometers and interferometry techniques to measure absolute RI, group RI, temperature, liquid flow rate and humidity are included. In addition, common latest models of fibre-optic interferometry sensors using in-fibre interferometer build are presented as well.

2.1 Overview of Refractive Index and Concentration Measurement

In optics, the RI or index of refraction is a dimensionless number that describes the propagation of electromagnetic radiation through a medium. The RI is a fundamental physical property of substances, which is dependent on chemical composition, electromagnetic radiation wavelength, humidity and ambient temperature. Precise measurement of RI can be used to derive the aforementioned physical parameters and monitor chemical modifications, which is particularly useful in analytic chemistry and biochemistry studies. Researchers are able to determine solute concentration in aqueous solutions or control the adulteration of liquids. Knowledge of the RI of aqueous solutions of salts and biological agents is of crucial importance in applications of evanescent wave techniques in biochemistry.

One of the most common techniques of RI and aqueous solution concentration measurement is using liquid prism. The involved method shows the measurement of deviated angle and path after incident laser light passed through the prism, where the incident light will get refracted to a degree depending on the RI of the testing sample (Sateesh, 2013; Yunus & Rahman, 1988).

Chemical modifications may be able to be detected by measurements of RI (Fan, 1998). The RI of sucrose, sodium chloride, glucose and caster sugar solutions for a range of density varying from distilled water to a saturated condition were measured. Through the refraction measurement, the concentrations of the medium can be determined (Yunus & Rahman, 1988). In the process of conducting the studies, possible sources of error are (i) temperature fluctuation during measurements on the samples, (ii) error in making up the solutions, and (iii) error in measurements of X and L (Ananth & Kleinbaum, 1997).

In some of the developed measuring device, the laser beam used as the light source is optically connected to a linear image sensor through a thin-walled cylindrical cuvette containing the liquid. Light beam undergoes vector displacement from their initial geometrical path, and captured by photodiode to measure the rate of displacement in order to determine the RI (Nemoto, 1992). However, such device suffers a rather low resolution and sensitivity of the optical measuring element, whose improvement requires enlargement of the dimensions of the device. Compared with conventional cuvette-type devices for measuring the RI of the liquids, the developed optical systems has proven to be more suitable and promising for the design of compact, accurate and stable devices for the control and analysis of both immobile and flowing liquids (Vilitis, Shipkovs, & Merkulov, 2009). Further development of RI measurement system based on beam displacement by angle concept has been done by Zhang *et al.*, (2014), Shurulinkov *et al.*, (1999), and Shelton, (2011) featuring an addition rotational and translational stage holding cuvette full with measuring samples to enable more manipulating variable control over RI measurement by changing the incident angle of beam light, opting for different angle displacement degree depending on the samples.

2.2 Interferometer Systems for Parameters Measurement

An interferometer is an optical device which utilizes the effect of interference to observe measurements. It typically starts with an input beam, splits it into two separate beams with a beam splitter, exposes some of these beams to external influences i.e. length changes or RI changes in a transparent medium, and recombines the beams on another beam splitter. The spatial shape power of the resulting beam is then used for parameter measurement and calculations. The ability of interferometers to detect small differences of optical path lengths in substances make them as some of the great devices to measure RI differences (Chen, Yang, & Chang, 2007).

Updated version of an in-depth review work by Bommarreddi regarding interferometer variants for measurement of changes in RI, temperature, concentration of materials for application in crystal growth rate, roughness, thermodynamic entropy exchange of materials in solid form, and etc. has been providing comprehensive knowledge of interferometry application, connecting other branches field of Physics (Bommarreddi, 2014). The following section discusses the popular configurations of interferometers.

2.2.1 Fabry-Pérot Interferometer

A basic schematic of the Fabry-Pérot Interferometer (FPI) is illustrated in Figure 2.2, its structure consisting of two parallel mirrors, allowing for multiple round trips of light. Coupled with highly reflective mirrors, the FPI configuration can have very sharp resonances, i.e. exhibit high transmission only for optical frequencies that

match certain values. Based on precise measurements of the resonant frequencies, distances can be determined at higher resolutions than the original wavelength.

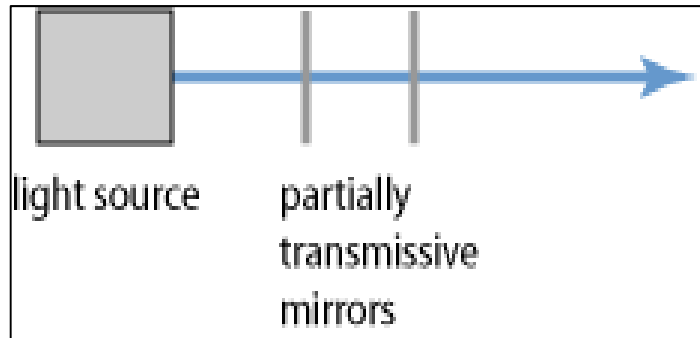


Figure 2.1 Fabry-Pérot Interferometer

FPI RI sensors have two main measurement types: one based on the wavelength shift of the sensor; the other based on the Fresnel reflection at the fibre's cleared end. Recent studies utilize both to simultaneously measure RI and temperature. Wang and Wang, (2012) spliced together a single-mode fibre and a photonic crystal fibre while using an in fibre ellipsoidal air-microcavity as the sensor head. The reflection intensities between the interfaces of between air-fibre, fibre-fibre, and solution fibre are used to determine the RI; while the amount of spectrum wavelength shifts due to thermo-optic properties of the fibre determine the temperature. Zhang *et al.*, (2014) demonstrated an end-of-fibre polydimethylsiloxane (PDMS) cap based FPI operating on the same principle. The PDMS cap provides advantages of hydrophobicity, good transparency, non-toxicity, and ease of synthesis; while allowing detection probe scans for biochemical application.

Another common FPI based interferometry sensor is through the dual-wavelength interference method, the thickness and the RI of transparent plate can be measured. The transmitted intensity versus angle of incidence is analyzed in this study through the fringes caused by the Fabry-Perot type interference. By using two